

## LETTERS

# Molecular architecture and assembly of the DDB1-CUL4A ubiquitin ligase machinery

Stephane Angers<sup>1,2\*</sup>†, Ti Li<sup>2\*</sup>, Xianhua Yi<sup>2</sup>, Michael J. MacCoss<sup>3</sup>, Randall T. Moon<sup>1,2,4</sup> & Ning Zheng<sup>2</sup>

Protein ubiquitination is a common form of post-translational modification that regulates a broad spectrum of protein substrates in diverse cellular pathways<sup>1</sup>. Through a three-enzyme (E1–E2–E3) cascade, the attachment of ubiquitin to proteins is catalysed by the E3 ubiquitin ligase, which is best represented by the superfamily of the cullin-RING complexes<sup>2,3</sup>. Conserved from yeast to human, the DDB1–CUL4–ROC1 complex is a recently identified cullin-RING ubiquitin ligase, which regulates DNA repair<sup>4–10</sup>, DNA replication<sup>11–14</sup> and transcription<sup>15</sup>, and can also be subverted by pathogenic viruses to benefit viral infection<sup>16</sup>. Lacking a canonical SKP1-like cullin adaptor and a defined substrate recruitment module, how the DDB1–CUL4–ROC1 E3 apparatus is assembled for ubiquitinating various substrates remains unclear. Here we present crystallographic analyses of the virally hijacked form of the human DDB1–CUL4A–ROC1 machinery, which show that DDB1 uses one  $\beta$ -propeller domain for cullin scaffold binding and a variably attached separate double- $\beta$ -propeller fold for substrate presentation. Through tandem-affinity purification of human DDB1 and CUL4A complexes followed by mass spectrometry analysis, we then identify a novel family of WD40-repeat proteins, which directly bind to the double-propeller fold of DDB1 and serve as the substrate-recruiting module of the E3. Together, our structural and proteomic results reveal the structural mechanisms and molecular logic underlying the assembly and versatility of a new family of cullin-RING E3 complexes.

Distinct from all known cullin adaptors, DDB1 is a large multi-domain protein featuring an independent  $\beta$ -propeller (BP) domain (BPB) flexibly connected to a clam-shaped double-propeller fold (BPA–BPC)<sup>17</sup>. To reveal how DDB1 incorporates into the CUL4A–ROC1 complex and mediates substrate recruitment, we determined the 3.1 Å crystal structure of a DDB1–CUL4A–ROC1 complex bound to the V protein of simian virus 5 (SV5-V), previously known as the VDC complex (Table 1). By docking the STAT proteins to DDB1, the V protein of the paramyxovirus is able to accelerate the ubiquitination

and degradation of STAT1, thereby blocking the antiviral response of the host<sup>16</sup>. With all the components in their full-length forms, the 240 kDa quaternary protein complex represents a functionally complete form of the E3 apparatus.

The DDB1–CUL4A–ROC1–SV5-V complex has an overall elongated shape that is about 170 Å long and 100 Å wide, resembling SCF (SKP1–cullin–F-box-protein)<sup>18</sup> (Fig. 1). As a close paralogue of CUL1, CUL4A adopts a CUL1-like structure with an arc-shaped

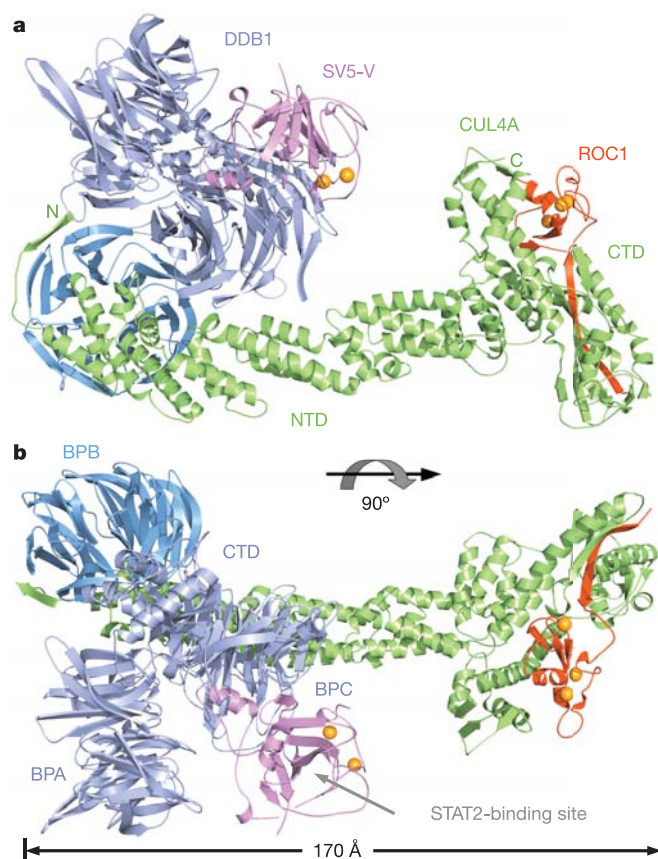


**Figure 1 | Crystal structure of the DDB1–CUL4A–ROC1 ubiquitin ligase complex hijacked by the V protein of simian virus 5.** **a, b**, Two orthogonal views of the complex structure are shown in ribbon diagram. DDB1, CUL4A, ROC1 and SV5-V are coloured in blue, green, red and magenta, respectively. The BPB domain of DDB1 is coloured in cyan. The zinc atoms in ROC1 and SV5-V are represented as orange spheres. A previously identified STAT2-binding site<sup>17</sup> of the viral protein, as well as the four domains of DDB1, are indicated.

**Table 1 | X-ray refinement statistics**

Resolution (Å)	3.1
$R_{work}$ ; $R_{free}$ (%)	25.1; 31.6
Number of atoms	
Protein	16,937
Ligand/ion	5
Water	0
B-factors	
Protein	75.9
Ligand/ion	93.5
Water	NA
Root-mean-squared deviations	
Bond lengths (Å)	0.008
Bond angles (°)	1.57

<sup>1</sup>Howard Hughes Medical Institute, <sup>2</sup>Department of Pharmacology, <sup>3</sup>Department of Genome Sciences, <sup>4</sup>Institute for Stem Cell and Regenerative Medicine, University of Washington, School of Medicine, Box 357280, Seattle, Washington 98195, USA. †Present address: Leslie Dan Faculty of Pharmacy, University of Toronto, Toronto, Ontario M5S 3M2, Canada. \*These authors contributed equally to this work.

helical amino-terminal domain (NTD) and a globular carboxy-terminal domain (CTD). Lacking the SKP1/BTB fold, DDB1 devotes its entire BPB domain for CUL4A binding, anchoring at the tip of the NTD of cullin. The BPA–BPC double-propeller fold of DDB1, however, is positioned in the complex facing towards the E2-binding subunit of the E3 ligase, ROC1. As a result, the viral protein—which sits at the opening of the large pocket of the DDB1 double-propeller fold—is about 45 Å away from the RING finger subunit. By comparing this overall architecture of the virally hijacked DDB1–CUL4A–ROC1 complex with SCF<sup>18</sup>, we conclude that the cullin-docking function and the substrate-presenting function of DDB1 are separately performed by the BPB domain and the BPA–BPC double-propeller fold, respectively.

The complex formation between DDB1 and CUL4A is predominantly mediated through two separate interfaces, both involving the BPB domain of DDB1 (Fig. 2a). At one interface, the top surface of the propeller fold of DDB1–BPB is recognized by the H2 and H5 helices of CUL4A, which are unexpectedly the same ones used by CUL1 to bind SKP1<sup>18</sup> (compare Fig. 2b, c). At the other interface, CUL4A further embraces the BPB domain of DDB1 using an N-terminal extension sequence, which is unique among all cullin family members<sup>17</sup>. Running across two blades of DDB1–BPB, this CUL4A N-terminal sequence wraps around the propeller of DDB1 at the peripheral side via a hydrogen-bond network and hydrophobic packing (Fig. 2a, d). The equal importance of these two separate interfaces in DDB1–CUL4A binding is reflected in the strict conservation of most of the interacting residues among CUL4 and DDB1 orthologues (Supplementary Fig. 1). Furthermore, mutations of the DDB1 or CUL4A residues involved in either interface can significantly weaken the complex formation<sup>13,17</sup>. Overall, the bipartite binding mode between DDB1 and CUL4A not only strongly supports a specific role of DDB1 in the CUL4A-based E3 machinery, but also demonstrates a surprising variation in cullin–adaptor interactions.

The crystal structures of DDB1 alone and in complex with SV5-V have previously revealed two distinct structural states of DDB1<sup>17</sup>, which show dramatic differences in the relative orientation between the substrate-presenting BPA–BPC double-propeller fold and the cullin-binding BPB domain. In the quaternary-complex crystal, DDB1 adopts yet a new domain arrangement. Intriguingly, super-

position analysis of the three structures indicates that all three domain configurations of DDB1 are in fact geometrically allowed in the context of the full DDB1–CUL4A–ROC1 complex (Fig. 2e). The BPA–BPC double-propeller folds of DDB1 in the resulting three models all similarly point towards the E2-binding RING subunit, even though the orientations of the fold itself are correlated by large degrees of rotation (compare Figs 1b and 2e). Because the BPA–BPC double-propeller fold of DDB1 has a very limited number of contacts with the cullin scaffold (Supplementary Fig. 2), we speculate that on binding to different cellular factors, DDB1 might be able to undergo conformational changes, which can modulate the ubiquitin ligase activity of the E3 machinery.

Although a multidomain structure might allow DDB1 to directly recruit substrates to the E3 platform, ubiquitination of several known DDB1–CUL4A substrates has been shown to require additional cellular factors<sup>7,19</sup>. Mimicked by the viral V protein, endogenous substrate-specific receptors might be used by DDB1 to expand its substrate repertoire. To further clarify the substrate targeting mechanisms of the DDB1–CUL4A E3 machinery, we used a proteomic approach optimized for isolating CUL4A and DDB1 protein complexes from mammalian cells by tandem-affinity purification<sup>20</sup>. In these analyses, more than 30 proteins were consistently identified by mass spectrometry, giving rise to a protein–interaction network shown in Fig. 3a.

Notably, besides several known cullin regulators and DDB1-binding proteins, numerous novel protein factors were identified in both the CUL4A and DDB1 complexes. In particular, a group of 16 proteins, including DDB2 and CSA, clearly stands out by sharing a predicted WD40 domain. The consistent presence and abundance of these WD40 proteins in the complexes strongly suggest that they represent bona fide members of the human DDB1–CUL4A E3 machinery (Supplementary Tables 2 and 3). It is also of note that reciprocal tandem-affinity pull-down analyses with DDB2 and two randomly selected WD40 proteins (H326 and WDTC1) confirmed that they are individually associated with the DDB1–CUL4A complex (Fig. 3a). Because many of these WD40 proteins do not have any known function other than DDB1–CUL4A binding, we propose to name them the DCAF (DDB1–CUL4A-associated factor) proteins (Supplementary Table 2).

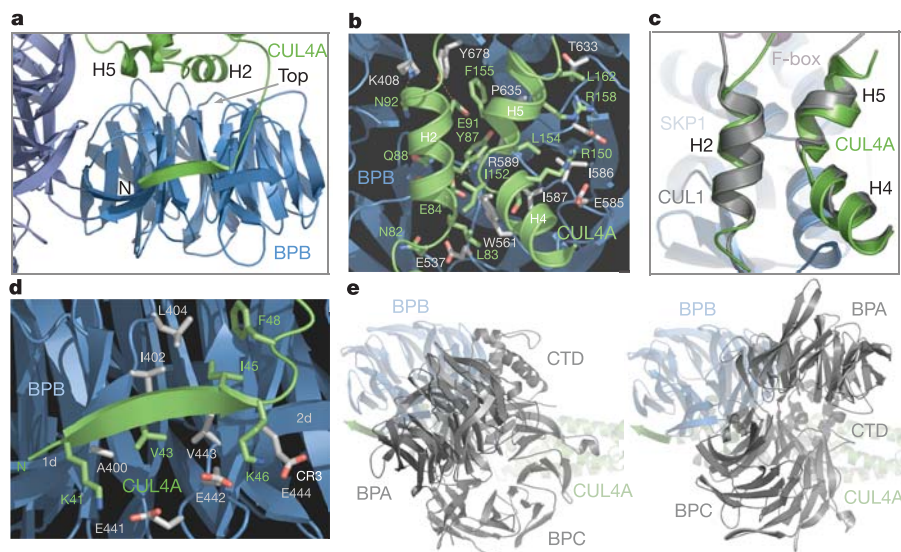


**Figure 2 | Binding interfaces and structural flexibility of DDB1 on CUL4A.** **a**, An overall view of the structural elements mediating the binding of the DDB1 BPB domain (cyan) with the CUL4A NTD (green). **b**, The interface between the top surface of DDB1–BPB (cyan) and the H2–H5 helices of CUL4A (green) viewed from above with participating side chains shown as sticks (grey in DDB1 and green in CUL4A). **c**, Superposition of the H2–H5 helices of CUL4A (green) and CUL1 (grey) with CUL1-bound SKP1 (blue)

shown in the background. The view is the same as that shown in panel **b**. CUL4A-bound DDB1 is not shown for clarity. **d**, The interface between the CUL4A N-terminal extension sequence (green) and the peripheral side of the DDB1 BPB domain (blue). **e**, Superposition analyses of DDB1 alone (right) and DDB1–SV5–V complex (left) structures in the context of the full DDB1–CUL4A–ROC1 complex. The models are docked through the BPB domain and viewed from the same angles as shown in Fig. 1b.



architecture of the virally hijacked DDB1–CUL4A–ROC1 complex strongly suggests that such a site might be located on the BPA–BPC double-propeller fold of DDB1, probably occupied by SV5-V, even though the viral protein does not have a WD40 domain. In fact, in an *in vitro* binding assay, association of DDB1 and two representative DCAF proteins, WDR23 (DCAF11) and WDTC1 (DCAF9) (data not shown), can be stoichiometrically competed off by increasing amounts of purified SV5-V protein (Fig. 3e). This *in vitro* result is consistent with a previous report showing that the same viral protein can compete with DDB2 for binding with DDB1<sup>26</sup>. It is interesting to note that, in order to anchor itself to DDB1, the viral protein not only binds to the surface of the BPA–BPC double-propeller fold of DDB1, but also inserts an entire helix into the large pocket of the DDB1 double-propeller fold. Although the size and secondary structure elements of a regular WD40 domain do not allow it to do so, it remains possible that some DCAF proteins might use sequence regions outside their WD40 domains to bind to the pocket of the DDB1 double-propeller fold, thereby further securing their associations with the CUL4A adaptor. Such an assembly mode could be used by the few DCAF proteins that lack a perfect double D<sub>x</sub>R box motif. Exactly how the DCAF proteins are docked to DDB1 awaits future structural studies.

As gene expression varies in different cell types and under different cellular states, the DCAF proteins identified in our studies are not expected to represent the complete family of substrate receptors of the DDB1–CUL4A E3 in human cells. Having established the structural and molecular basis of the assembly of the E3 machinery, our studies pave the road for a future understanding of the functions of the DDB1–CUL4A complex in eukaryotic biology and in human diseases.

## METHODS

**Protein preparation.** Human CUL4A and ROC1 were co-expressed and purified from *Escherichia coli* and mixed with previously purified DDB1 and SV5-V<sup>17</sup>. WDR23 (DCAF11) (amino-acid residues 39–546) and H326 (DCAF8) (amino-acid residues 177–555) were overexpressed and purified from *E. coli* as GST-fusion proteins.

**Crystallography.** The VDC-complex crystals were grown at 4 °C by the hanging-drop diffusion method. The crystals grew from 100 mM NaHEPES, 7–9% (w/v) PEG 4000, 10% (v/v) isopropanol, 5 mM dithiothreitol, pH 8.0. A native data set was collected at the 8.2.2 beamline at the Advanced Light Source in Berkeley, California, using a crystal flash-frozen in the crystallization buffer supplemented with 20% (v/v) 2-methyl-2,4-pentanediol (MPD) at –170 °C. The crystal forms in space group C222<sub>1</sub>, with  $a = 83.46 \text{ \AA}$ ,  $b = 203.19 \text{ \AA}$ ,  $c = 424.87 \text{ \AA}$ , and one complex in the asymmetric unit. For further details, see Supplementary Methods and Supplementary Fig. 5.

**Tandem-affinity purification.** Tandem-affinity purification (TAP) and mass spectrometry analyses of the DDB1 and CUL4A protein complexes were performed using HEK293T cells stably expressing the TAP-tagged constructs. The detailed protocol has been described previously<sup>20</sup>.

**Co-affinity purification and GST pull-down assay.** Co-affinity purifications were performed using HEK293T cells stably expressing pGLUE-DDB1. Cells were transfected with different Flag-tagged DCAF proteins using CaPO<sub>4</sub>. Forty-eight hours post-transfection, cells were lysed using stringent radio-immunoprecipitation buffer (RIPA; 25 mM Tris-HCl, pH 8.0, 250 mM NaCl, 10% (v/v) glycerol, 1% (v/v) Igepal CA-630, 0.25% (w/v) deoxycholic acid, 2 mM EDTA, 1 mM NaF, 50 mM β-glycerophosphate). Lysates were cleared by centrifugation and affinity purification was performed using sepharose–streptavidin resin (Amersham). Anti-Flag M2 antibody (F1804; Sigma) and anti-haemagglutinin (HA) antibody (3F10; Roche) were used to detect the Flag-tagged DCAF proteins and DDB1, respectively. Previously reported procedures<sup>18</sup> were followed for the *in vitro* GST pull-down experiments except that the final samples were analysed by western blot analysis using an anti-DDB1 antibody (ab13562; abcam).

Received 15 June; accepted 17 August 2006.

Published online 10 September 2006.

- Hershko, A. & Ciechanover, A. The ubiquitin system. *Annu. Rev. Biochem.* **67**, 425–479 (1998).
- Pickart, C. M. Mechanisms underlying ubiquitination. *Annu. Rev. Biochem.* **70**, 503–533 (2001).
- Petroski, M. D. & Deshaies, R. J. Function and regulation of cullin-RING ubiquitin ligases. *Nature Rev. Mol. Cell Biol.* **6**, 9–20 (2005).
- Nag, A., Bondar, T., Shiv, S. & Raychaudhuri, P. The xeroderma pigmentosum group E gene product DDB2 is a specific target of cullin 4A in mammalian cells. *Mol. Cell. Biol.* **21**, 6738–6747 (2001).
- Chen, X., Zhang, Y., Douglas, L. & Zhou, P. UV-damaged DNA-binding proteins are targets of CUL-4A-mediated ubiquitination and degradation. *J. Biol. Chem.* **276**, 48175–48182 (2001).
- Sugasawa, K. *et al.* UV-induced ubiquitylation of XPC protein mediated by UV-DDB-ubiquitin ligase complex. *Cell* **121**, 387–400 (2005).
- Groisman, R. *et al.* CSA-dependent degradation of CSB by the ubiquitin–proteasome pathway establishes a link between complementation factors of the Cockayne syndrome. *Genes Dev.* **20**, 1429–1434 (2006).
- Groisman, R. *et al.* The ubiquitin ligase activity in the DDB2 and CSA complexes is differentially regulated by the COP9 signalosome in response to DNA damage. *Cell* **113**, 357–367 (2003).
- Kapetanaki, M. G. *et al.* The DDB1–CUL4A<sup>DDB2</sup> ubiquitin ligase is deficient in xeroderma pigmentosum group E and targets histone H2A at UV-damaged DNA sites. *Proc. Natl Acad. Sci. USA* **103**, 2588–2593 (2006).
- Wang, H. *et al.* Histone H3 and H4 ubiquitylation by the CUL4–DDB–ROC1 ubiquitin ligase facilitates cellular response to DNA damage. *Mol. Cell* **22**, 383–394 (2006).
- Liu, C. *et al.* Cop9/signalosome subunits and Pcu4 regulate ribonucleotide reductase by both checkpoint-dependent and -independent mechanisms. *Genes Dev.* **17**, 1130–1140 (2003).
- Higa, L. A., Mihaylov, I. S., Banks, D. P., Zheng, J. & Zhang, H. Radiation-mediated proteolysis of CDT1 by CUL4–ROC1 and CSN complexes constitutes a new checkpoint. *Nature Cell Biol.* **5**, 1008–1015 (2003).
- Hu, J., McCall, C. M., Ohta, T. & Xiong, Y. Targeted ubiquitination of CDT1 by the DDB1–CUL4A–ROC1 ligase in response to DNA damage. *Nature Cell Biol.* **6**, 1003–1009 (2004).
- Bondar, T., Ponomarev, A. & Raychaudhuri, P. Ddb1 is required for the proteolysis of the *Schizosaccharomyces pombe* replication inhibitor Spd1 during S phase and after DNA damage. *J. Biol. Chem.* **279**, 9937–9943 (2004).
- Wertz, I. E. *et al.* Human De-etiolated-1 regulates c-Jun by assembling a CUL4A ubiquitin ligase. *Science* **303**, 1371–1374 (2004).
- Horvath, C. M. Weapons of STAT destruction. Interferon evasion by paramyxovirus V protein. *Eur. J. Biochem.* **271**, 4621–4628 (2004).
- Li, T., Chen, X., Garbutt, K. C., Zhou, P. & Zheng, N. Structure of DDB1 in complex with a paramyxovirus V protein: viral hijack of a propeller cluster in ubiquitin ligase. *Cell* **124**, 105–117 (2006).
- Zheng, N. *et al.* Structure of the Cul1–Rbx1–Skp1–F box<sup>Skp2</sup> SCF ubiquitin ligase complex. *Nature* **416**, 703–709 (2002).
- Liu, C. *et al.* Transactivation of *Schizosaccharomyces pombe* *cdt2*<sup>+</sup> stimulates a Pcu4–Ddb1–CSN ubiquitin ligase. *EMBO J.* **24**, 3940–3951 (2005).
- Angers, S. *et al.* The KLHL12–Cullin-3 ubiquitin ligase negatively regulates the Wnt–β-catenin pathway by targeting Dishevelled for degradation. *Nature Cell Biol.* **8**, 348–357 (2006).
- Lambright, D. G. *et al.* The 2.0 Å crystal structure of a heterotrimeric G protein. *Nature* **379**, 311–319 (1996).
- Wall, M. A. *et al.* The structure of the G protein heterotrimer G<sub>αi1</sub>βγ<sub>2</sub>. *Cell* **83**, 1047–1058 (1995).
- Shiyanov, P. *et al.* The naturally occurring mutants of DDB are impaired in stimulating nuclear import of the p125 subunit and E2F1-activated transcription. *Mol. Cell. Biol.* **19**, 4935–4943 (1999).
- Li, F. *et al.* Two novel proteins, dos1 and dos2, interact with rik1 to regulate heterochromatic RNA interference and histone modification. *Curr. Biol.* **15**, 1448–1457 (2005).
- Thon, G. *et al.* The Clr7 and Clr8 directionality factors and the Pcu4 cullin mediate heterochromatin formation in the fission yeast *Schizosaccharomyces pombe*. *Genetics* **171**, 1583–1595 (2005).
- Leupin, O., Bontron, S. & Strubin, M. Hepatitis B virus X protein and simian virus 5 V protein exhibit similar UV-DDB1 binding properties to mediate distinct activities. *J. Virol.* **77**, 6274–6283 (2003).

**Supplementary Information** is linked to the online version of the paper at [www.nature.com/nature](http://www.nature.com/nature).

**Acknowledgements** We thank the beamline staff of the Advanced Light Source at Berkeley for help with data collection, P. Zhou, W. Xu, J. Beavo, Z. Gao and members of the Zheng and Moon laboratories for discussions and help. We also thank J. W. Harper and Y. Xiong for communicating unpublished results. This work is supported by grants from the National Institutes of Health (to N.Z. and M.J.M.), the Pew Scholar Program (N.Z.), and the Howard Hughes Medical Institute (S.A. and R.T.M.).

**Author Contributions** S.A. and T.L. contributed equally to this work.

**Author Information** Structure coordinates for the DDB1–CUL4A–ROC1–SV5-V complex have been deposited in the Protein Data Bank under accession number 2HYE. Reprints and permissions information is available at [www.nature.com/reprints](http://www.nature.com/reprints). The authors declare no competing financial interests. Correspondence and requests for materials should be addressed to N.Z. (nzheng@u.washington.edu) or R.T.M. (rtmoon@u.washington.edu).